Advances in Electronics and Electron Physics

EDITED BY
PETER W. HAWKES

VOLUME 61

Advances in Electronics and Electron Physics

EDITED BY

PETER W. HAWKES

Laboratoire d'Optique Electronique
du Centre National de la Recherche Scientifique
Toulouse, France

ACADEMIC PRESS
A Subsidiary of Harcourt Brace Jovanovich, Publishers
New York London
Paris San Diego San Francisco São Paulo Sydney Tokyo Toronto

ACADEMIC PRESS, INC.
111 Fifth Avenue, New York, New York 10003

United Kingdom Edition published by
ACADEMIC PRESS, INC. (LONDON) LTD.
24/28 Oval Road, London NW1 7DX

LIBRARY OF CONGRESS CATALOG CARD NUMBER: 49-7504

ISBN 0-12-014661-4

PRINTED IN THE UNITED STATES OF AMERICA

83 84 85 86 9 8 7 6 5 4 3 2 1

CONTRIBUTORS TO VOLUME 61

Numbers in parentheses indicate the pages on which the authors' contributions begin.

H. BREMMER, 31 Bosuillaan, Flatgebouw Houdringe, Bilthoven, The Netherlands (299)

D. S. BUGNOLO,* Department of Electrical and Computer Engineering, Florida Institute of Technology, Melbourne, Florida 32901 (299)

M. CAILLER, Laboratoire de Physique du Métal, Ecole Nationale Supérieure de Mécanique, 44072 Nantes Cedex, France (161)

GILBERT DE MEY, Laboratory of Electronics, Ghent State University, B-9000 Ghent, Belgium (1)

J. P. GANACHAUD, Laboratoire de Physique du Solide, Institut de Physique de l'Université de Nantes, Nantes, France (161)

A. G. MILNES, Department of Electrical Engineering, Carnegie-Mellon University, Pittsburgh, Pennsylvania 15213 (63)

D. ROPTIN, Laboratoire de Physique du Métal, Ecole Nationale Supérieure de Mécanique, 44072 Nantes Cedex, France (161)

*Present address: Department of Electrical and Computer Engineering, University of Alabama in Huntsville, Huntsville, Alabama 35899.

Waveguide and Coaxial Probes for Nondestructive Testing of Materials	F. E. Gardiol
The Measurement of Core Electron Energy Levels	R. N. Lee and C. Anderson
Millimeter Radar	Robert D. Hayes
Recent Advances in the Theory of Surface Electronic Structure	Henry Krakauer
Long-Life High-Current-Density Cathodes	Robert T. Longo
Microwaves in Semiconductor Electronics	J. L. Allen
Applications of Quadrupole Mass Spectrometers	I. Berecz, S. Bohatka, and G. Langer
Advances in Materials for Thick-Film Hybrid Microcircuits	J. Sergent
Guided-Wave Circuit Technology	M. K. Barnoski
Fast-Wave Tube Devices	J. M. Baird
Spin Effects in Electron–Atom Collision Processes	H. Kleinpoppen
Recent Advances in and Basic Studies of Photoemitters	H. Timan
Solid State Imaging Devices	E. H. Snow
Structure of Intermetallic and Interstitial Compounds	A. C. Switendick
Smart Sensors	W. G. Wolber
Structure Calculations in Electron Microscopy	D. van Dyck
Voltage Measurements in the Scanning Electron Microscope	A. Gopinath

Supplementary Volumes:

Microwave Field-Effect Transistors	J. Frey
Magnetic Reconnection	P. J. Baum and A. Bratenahl

Volume 62:

Predictions of Deep Impurity-Level Energies in Semiconductors	P. Vogl
Spin-Polarized Electrons in Solid-State Physics	H. C. Siegmann, F. Meier, M.Erbudak, and M. Landolt
Recent Advances in the Electron Microscopy of Materials	D. B. Williams and D.E. Newbury

PETER W. HAWKES

CONTRIBUTORS TO VOLUME 61

Numbers in parentheses indicate the pages on which the authors' contributions begin.

H. BREMMER, 31 Bosuillaan, Flatgebouw Houdringe, Bilthoven, The Netherlands (299)

D. S. BUGNOLO,* Department of Electrical and Computer Engineering, Florida Institute of Technology, Melbourne, Florida 32901 (299)

M. CAILLER, Laboratoire de Physique du Métal, Ecole Nationale Supérieure de Mécanique, 44072 Nantes Cedex, France (161)

GILBERT DE MEY, Laboratory of Electronics, Ghent State University, B-9000 Ghent, Belgium (1)

J. P. GANACHAUD, Laboratoire de Physique du Solide, Institut de Physique de l'Université de Nantes, Nantes, France (161)

A. G. MILNES, Department of Electrical Engineering, Carnegie-Mellon University, Pittsburgh, Pennsylvania 15213 (63)

D. ROPTIN, Laboratoire de Physique du Métal, Ecole Nationale Supérieure de Mécanique, 44072 Nantes Cedex, France (161)

*Present address: Department of Electrical and Computer Engineering, University of Alabama in Huntsville, Huntsville, Alabama 35899.

CONTENTS

Contributors to Volume 61 vii
Foreword ix

Potential Calculations in Hall Plates
Gilbert De Mey

I. Introduction 2
II. Fundamental Equations for a Hall-Plate Medium 3
III. The Van Der Pauw Method. 7
IV. Influence of the Geometry on Hall-Mobility Measurements . . . 9
V. Conformal Mapping Techniques. 10
VI. Relaxation Methods 15
VII. The Boundary-Element Method for Potential Calculations in Hall Plates 18
VIII. Improvement of the Boundary-Element Method 38
IX. Conclusion 48
Appendix 1. The Three-Dimensional Hall Effect 49
Appendix 2. On the Existence of Solutions of Integral Equations 52
Appendix 3. Green's Theorem 54
Appendix 4. The Hall-Effect Photovoltaic Cell 57
Appendix 5. Contribution of the Hall-Plate Current to the Magnetic Field 58
Appendix 6. Literature 59
References 59

Impurity and Defect Levels (Experimental) in Gallium Arsenide
A. G. Milnes

I. Introduction 64
II. Possible Native Defects and Complexes 65
III. Traps (and Nomenclature) from DLTS Studies 76
IV. Levels Produced by Irradiation 81
V. Semi-Insulating Gallium Arsenide with and without Chromium . . 91
VI. Effects Produced by Transition Metals. 100
VII. Group I Impurities: Li, Cu, Ag, Au 108
VIII. Shallow Acceptors: Be, Mg, Zn, Cd. 116
IX. Group IV Elements as Dopants: C, Si, Ge, Sn, Pb 118
X. Oxygen in GaAs. 123

XI. Group VI Shallow Donors: S, Se, Te 127
XII. Other Impurities (Mo, Ru, Pd, W, Pt, Tm, Nd) 128
XIII. Minority-Carrier Recombination, Generation, Lifetime, and Diffusion Length 131
XIV. Concluding Discussion 141
References 142

Quantitative Auger Electron Spectroscopy

M. CAILLER, J. P. GANACHAUD, AND D. ROPTIN

I. Introduction 162
II. General Definitions 167
III. Dielectric Theory of Inelastic Collisions of Electrons in a Solid . . 173
IV. Elastic Collisions 185
V. Auger Transitions in a Solid 187
VI. Quantitative Description of Auger Emission 213
VII. Auger Quantitative Analysis 244
VIII. Conclusion 289
References 289

The Wigner Distribution Matrix for the Electric Field in a Stochastic Dielectric with Computer Simulation

D. S. BUGNOLO AND H. BREMMER

I. Introduction 300
II. The Differential Equation for the Electric Field Correlations . . . 303
III. Derivation of the Equations for the Wigner Distribution Functions 313
IV. Related Equations for the Wigner Distribution Function 325
V. Asymptotic Equations for the Wigner Distribution Function . . . 330
VI. Equations for Some Special Cases 335
VII. A Brief Review of Other Theoretical Methods 345
VIII. The Coherent Wigner Function 347
IX. Computer Simulation of the Stochastic Transport Equation for the Wigner Function in a Time-Invariant Stochastic Dielectric 354
X. Conclusions 382
Appendix 1. A Listing of Experimental Program Number Two for the Case of an Exponential Space Correlation Function . . . 383
Appendix 2. A Sample of a Computer Simulation 386
References 388

AUTHOR INDEX 391
SUBJECT INDEX 402

Potential Calculations in Hall Plates

GILBERT DE MEY

Laboratory of Electronics
Ghent State University
Ghent, Belgium

I.	Introduction	2
II.	Fundamental Equations for a Hall-Plate Medium	3
	A. General Equations for a Semiconductor	3
	B. Approximations for a Thin Semiconducting Layer	4
	C. Constitutive Relations with an Externally Applied Magnetic Field	5
	D. Boundary Conditions with Externally Applied Magnetic Field	6
III.	The Van Der Pauw Method	7
IV.	Influence of the Geometry on Hall-Mobility Measurements	9
V.	Conformal Mapping Techniques	10
	A. Basic Ideas	10
	B. Approximate Analysis of the Cross-Shaped Geometry	11
	C. Exact Analysis of the Cross-Shaped Sample	13
	D. Properties of the Cross-Shaped Hall Plate	14
VI.	Relaxation Methods	15
VII.	The Boundary-Element Method for Potential Calculations in Hall Plates	18
	A. Introduction	18
	B. Integral Equation for the Potential Distribution in a Hall Plate	18
	C. Numerical Solution of the Integral Equation	20
	D. Application to a Rectangular Hall Plate	21
	E. Zeroth-Order Approximation	22
	F. Numerical Calculation of the Current through a Contact	24
	G. Application to the Cross-Shaped Geometry	25
	H. Direct Calculation of the Geometry Correction	27
	I. Application to a Rectangular Hall Generator	29
	J. Application to a Cross-Shaped Geometry	30
	K. Application to Some Other Geometries	33
VIII.	Improvement of the Boundary-Element Method	38
	A. Introduction	38
	B. Integral Equation	39
	C. Calculation of the Functions $\varphi_i(\mathbf{r})$	40
	D. Application to a Rectangular Hall Generator	43
	E. Application to a Cross-Shaped Form	45
	F. Application to Some Other Geometries	46
IX.	Conclusion	48
	Appendix 1. The Three-Dimensional Hall Effect	49
	Appendix 2. On the Existence of Solutions of Integral Equations	52
	Appendix 3. Green's Theorem	54

ISBN 0-12-014661-4

Appendix 4. The Hall-Effect Photovoltaic Cell 57
Appendix 5. Contribution of the Hall-Plate Current to the Magnetic Field 58
Appendix 6. Literature 59
References 59

I. Introduction

Hall plates are thin semiconducting layers placed in a magnetic field. Owing to the Lorentz force, the current density **J** and the electric field **E** are no longer parallel vectors. This means that a current in a given direction automatically generates a potential gradient in the perpendicular direction. With suitable contacts (the so-called Hall contacts), a Hall voltage can then be measured. In a first approximation one can state that the Hall voltage is proportional to the applied magnetic field, the externally supplied current, and the mobility of the charge carriers. Knowledge of the current and of the Hall voltage yields the product $\mu_H B$ of the mobility μ_H and the magnetic field B. This indicates two major applications of Hall-effect components. If the mobility is known, magnetic field strengths can be measured. On the other hand, if the magnetic field is known, the mobility can be calculated. The latter is mainly used for the investigation of semiconductors because mobility is a fundamental material parameter.

A first series of applications is based on the measurement or detection of magnetic fields. Measurements of the magnetic fields in particle accelerators have been carried out with Hall probes provided with a special geometry in order to ensure a linear characteristic (Haeusler and Lippmann, 1968). Accuracies better than 0.1% have been realized. For alternating magnetic fields, Hall plates can be used at frequencies up to $\pm 10{,}000$ Hz (Bonfig and Karamalikis, 1972a,b). For higher frequencies emf measurements are recommended to measure magnetic fields. The Hall probe can also be used to detect the presence of a magnetic field. This phenomenon is used in some types of push buttons. On each button a small permanent magnet is provided, and the pushing is sensed by a Hall plate. At this writing Hall plates combined with additional electronic circuitry are available in integrated-circuit form. A Japanese company has produced a cassette recorder in which a Hall probe reads the magnetic tape. The principal advantage here is that dc signals can be read directly from a tape, whereas classical reading heads generate signals proportional to the magnetic flux rate $d\phi/dt$. Magnetic bubble memories have also been fitted out with Hall-effect readers (Thompson *et al.*, 1975).

A survey of Hall-effect applications can be found in an article written by Bulman (1966) that mentions microwave-power measurements, the use of Hall probes as gyrators, insulators, function generators, ampere meters, etc. Even a brushless dc motor has been constructed using the Hall effect (Kobus and Quichaud, 1970). Finally, Hall plates can also be applied as transducers for mechanical displacements (Davidson and Gourlay, 1966; Nalecz and Warsza, 1966).

A second series of applications, to which this article is mainly devoted, involves the measurement of mobilities. A Hall measurement carried out in a known magnetic field yields the value of μ_H. This constant is an important parameter for investigating the quality of semiconducting materials. Combined with the resistivity, it also enables us to calculate the carrier concentration. Knowledge of these data is necessary for the construction of components such as diodes, solar cells, and transistors starting from a semiconducting slice.

The present article describes the Hall effect and its mathematical representation. The well-known Van Der Pauw method for Hall-mobility measurements is then discussed. The influence of the geometry on the Hall voltage is pointed out using physical considerations. This explains why the potential distribution in a Hall plate should be known in order to evaluate the so-called geometry correction. Then several techniques for potential calculations in Hall plates, such as conformal mapping, finite differences, and the boundary-element method, are outlined and compared.

II. Fundamental Equations for a Hall-Plate Medium

A. General Equations for a Semiconductor

The fundamental equations for an n-type semiconductor (assuming low injection) are the following:

$$\begin{aligned}(\partial n/\partial t) - q^{-1}\nabla\cdot\mathbf{J}_n &= (\partial n/\partial t)_{\text{gen}} - [(p-p_0)/\tau_p]\\ (\partial p/\partial t) + q^{-1}\nabla\cdot\mathbf{J}_p &= (\partial p/\partial t)_{\text{gen}} - [(p-p_0)/\tau_p]\end{aligned} \tag{1}$$

(substitute $[(n-n_0)/\tau_n]$ for a p-type layer);

$$\mathbf{J}_n = nq\mu_n\mathbf{E} + qD_n\nabla n, \qquad \mathbf{J}_p = pq\mu_p\mathbf{E} - qD_p\nabla p \tag{2}$$

$$\nabla\cdot\mathbf{E} = -\nabla^2\phi = (q/\epsilon_0\epsilon)(p - n + N_D - N_A) \tag{3}$$

where n is the electron concentration, p is the hole concentration, $\mathbf{J}_n$ is the electron current density, $\mathbf{J}_p$ is the hole current density, $\mathbf{J} = \mathbf{J}_n + \mathbf{J}_p$ is the total current density, N_D is the donor concentration, N_A is the acceptor concentration, $\mathbf{E}$ is the electric field, ϕ is the electric poential, $\mu_n = qD_n/kT$ is the electron mobility, $\mu_p = qD_p/kT$ is the hole mobility, τ_n is the electron relaxation time, τ_p is the hole relaxation time, n_0 is the equilibrium electron concentration (in the p layer), p_0 is the equilibrium hole concentration

8550127

(in the n layer), ϵ is the dielectric constant, and $(\partial/\partial t)_{\text{gen}}$ is the generation rate (e.g., due to incident light). Equations (1)–(3) are nonlinear for the unknowns n, p, and ϕ; however, for Hall generators several reasonable assumptions can be advanced so that the final problem becomes linear.

B. *Approximations for a Thin Semiconducting Layer*

For thin-film semiconducting layers with contacts sufficiently distant from each other (order of magnitude in millimeters), one usually assumes that the layer is sufficiently doped to ensure that the contribution of the minority carriers becomes negligible. We shall work later with an n-type semiconductor; however, the same treatment can be carried out for a p-type semiconductor.

One also assumes that no space charges are built up in the conductor. It can be shown that an occasional space charge only has an influence over a distance comparable to the Debye length. For an n-type layer, the Debye length is given by (Many *et al.*, 1965)

$$L_D = [(\epsilon_0 \epsilon k T)/q^2 N_D)]^{1/2} \tag{4}$$

Normally, L_D varies around 100–1000 Å, so that a space charge can only be felt over a distance much smaller than the distance between the electrodes. Practically, space charges can only be realized at junctions or nonohmic contacts. Because Hall generators are provided with ohmic contacts, the space charge is zero everywhere. Hence the right-hand member of (3) should vanish; for an n-type material this gives rise to

$$n = N_D \qquad \text{and} \qquad p \ll n \tag{5}$$

The Poisson equation (3) is then reduced to the simpler Laplace equation

$$-\nabla \cdot \mathbf{E} = \nabla^2 \phi = 0 \tag{6}$$

From Eq. (5), it also follows that ∇n should be zero. This means that the current density $\mathbf{J}_n$ only consists of the drift component $q\mu_n n\mathbf{E}$. The hole current $\mathbf{J}_p$ can be put at zero because both p and ∇p are negligible. One obtains for the current density

$$\mathbf{J} = \mathbf{J}_n = N_D q \mu_n \mathbf{E} = \sigma \mathbf{E} \tag{7}$$

A thin semiconducting layer can be seen simply as a sheet with a constant conductivity σ.

For sufficiently high doping concentrations N_D, the minority-carrier concentration p can be put equal to its equilibrium value p_0, hence $p - p_0 = 0$. In the time-independent case, Eq. (1) reduces to

$$\nabla \cdot \mathbf{J} = \nabla \cdot \mathbf{J}_n = 0 \tag{8}$$

if we suppose that the generation term $(\partial n/\partial t)_{gen}$ vanishes, which will be the case if the layer is not illuminated or irradiated.

Equations (6) and (8) constitute the fundamental equations for a semiconducting layer, **J** and **E** being related by Eq. (7). From these equations, the boundary conditions can easily be deduced. At a metallic contact the potential ϕ should be equal to the applied voltage. At a free boundary the current density must be tangential:

$$\mathbf{J}\cdot\mathbf{u}_n = 0 \tag{9}$$

where $\mathbf{u}_n$ is the normal unit vector. Owing to Eq. (7), the boundary condition (9) is equivalent to

$$\nabla\phi\cdot\mathbf{u}_n = 0 \tag{10}$$

The potential problem in a thin semiconducting layer is reduced to the solution of the Laplace equation in a given geometry, ϕ or $\nabla\phi\cdot\mathbf{u}_n$ being known on each point along the boundary. This is a classical potential problem with mixed boundary conditions.

C. *Constitutive Relations with an Externally Applied Magnetic Field*

The fundamental equations (1) and (2) are still valid in the presence of an externally applied magnetic field. Only the constitutive relations (2) have to be extended in the following way (Smith *et al.*, 1967; Madelung, 1970):

$$J_{n,i} = \sum_j [nq\mu_{ij}E_j - q\mu_{ij}(kT/q)(\partial n/\partial x_j)] \tag{11}$$

where the index i denotes the ith component in a rectangular coordinate system. A similar expression can be written for the hole current density $J_{p,i}$. The tensorial mobility μ_{ij} in the presence of a magnetic field **B** is found by the well-known Jones–Zener expansion, and it turns out that μ_{ij} has to be replaced by

$$\mu_{ij} \rightarrow \mu_{ij} + \sum_k \mu_{ijk}B_k \tag{12}$$

Applying Eqs. (11) and (12) on a flat n-type semiconductor layer, one obtains (De Mey, 1975)

$$\mathbf{J} = \sigma\mathbf{E} + qD\,\nabla n - \sigma\mu_H(\mathbf{E}\times\mathbf{B}) - q\mu_H D(\nabla n\times\mathbf{B}) \tag{13}$$

Using the approximation (5), as has also been done in the foregoing section, the diffusion components in Eq. (13) can be dropped, which yields

$$\mathbf{J} = \sigma\mathbf{E} - \sigma\mu_H(\mathbf{E}\times\mathbf{B}) \tag{14}$$

This relation is used later for potential calculations in Hall plates. It has also been assumed that the semiconductor is isotropic, which explains why only one μ_H coefficient remains in Eq. (14).

Equation (14) is derived from the Jones–Zener expansion (12) neglecting terms of order $\mu_H^2 B^2$ that describe the physical magnetoresistivity. Hence Eq. (14) can be inverted to

$$\mathbf{E} = \rho \mathbf{J} + \rho \mu_H (\mathbf{J} \times \mathbf{B}) \tag{15}$$

where $\rho = 1/\sigma$ denotes the resistivity. Equation (15) is also correct to terms of order $\mu_H B$.

The fundamental equations are still $\nabla \cdot \mathbf{J} = 0$ and $\nabla \times \mathbf{E} = 0$, but for a flat semiconducting Hall plate in a uniform magnetic field **B**, one can show the following:

$$\nabla \cdot \mathbf{J} = \sigma \nabla \cdot \mathbf{E} - \sigma \mu_H \nabla \cdot (\mathbf{E} \times \mathbf{B}) = \sigma \nabla \cdot \mathbf{E} - \sigma \mu_H (\nabla \times \mathbf{E}) \cdot \mathbf{B} = \sigma \nabla \cdot \mathbf{E} = 0$$

$$\nabla \times \mathbf{J} = \sigma \nabla \times \mathbf{E} - \sigma \mu_H \nabla \times (\mathbf{E} \times \mathbf{B}) = -\sigma \mu_H (\mathbf{B} \cdot \nabla) \mathbf{E} + \sigma \mu_H (\nabla \cdot \mathbf{E}) \mathbf{B} = 0$$

in which $(\mathbf{B} \cdot \nabla)\mathbf{E}$ vanishes since **B** is directed perpendicular to the Hall plate, whereas **E** is parallel to it. To solve the problem one can use either $\nabla \times \mathbf{E} = \nabla \cdot \mathbf{E} = 0$ or $\nabla \times \mathbf{J} = \nabla \cdot \mathbf{J} = 0$; **E** can be derived from a potential ϕ. For reasons which are explained in Section II,D, the current density **J** can also be derived from a potential function ψ in the following way:

$$\mathbf{J} = \mathbf{u}_z \times \nabla \psi \tag{16}$$

where $\mathbf{u}_z$ is the unity vector directed perpendicular to the Hall plate. From $\nabla \times \mathbf{J} = 0$ it can be easily proved that ψ also satisfies the Laplace equation.

D. Boundary Conditions with an Externally Applied Magnetic Field

Let us start with the electrostatic potential ϕ. At a metallic contact ϕ is equal to the applied contact voltage. At a free boundary, the current density should be tangential:

$$\mathbf{J} \cdot \mathbf{u}_n = \sigma \mathbf{E} \cdot \mathbf{u}_n - \sigma \mu_H B \mathbf{E} \cdot \mathbf{u}_t = 0 \tag{17}$$

or

$$\nabla \phi \cdot \mathbf{u}_n = \mu_H B \nabla \phi \cdot \mathbf{u}_t \tag{18}$$

where $\mathbf{u}_t = \mathbf{u}_z \times \mathbf{u}_n$ is the unit tangential vector along the boundary (Fig. 1). It should be noted that at a free boundary in a Hall plate the electric field can show a nonvanishing normal component.

For a *p*-type semiconductor, the same calculations can be carried out. A minus sign will then appear in the right-hand member of Eq. (18).

For Hall plates the current but not the potential through a contact is usually given. It is then easier to introduce the current potential defined by Eq. (16). At a metallic contact **E** should be perpendicular, or the tangential

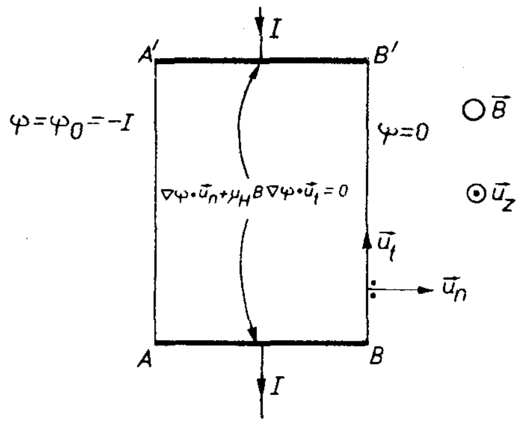

FIG. 1. Hall-plate configuration for outlining the stream potential.

component $\mathbf{E}\cdot\mathbf{u}_t$ must vanish. With Eq. (14) this gives rise to

$$\sigma \mathbf{E}\cdot\mathbf{u}_t = \mathbf{J}\cdot\mathbf{u}_t + \mu_H(\mathbf{J}\times\mathbf{B})\cdot\mathbf{u}_t = 0 \tag{19}$$

or

$$\nabla\psi\cdot\mathbf{u}_n + \mu_H B\,\nabla\psi\cdot\mathbf{u}_t = 0 \tag{20}$$

At a free boundary, $\mathbf{J}$ must be tangential, and due to Eq. (16) ψ must be a constant (Fig. 1).

At BB' the boundary value can be taken $\psi = 0$. At the opposite side AA', the value ψ_0 can be found from the known current I injected through the contacts:

$$I = -\int_{A'}^{B'} \mathbf{J}\cdot\mathbf{u}_n\,dl = \int_{A'}^{B'} \nabla\psi\cdot\mathbf{u}_t\,dl = \psi(B') - \psi(A') = -\psi_0 \tag{21}$$

A similar treatment can be performed if more than two contacts are involved.

III. The Van Der Pauw Method

Van Der Pauw (1958) has presented an ingenious method for carrying out resistivity and Hall-mobility measurements on thin layers with arbitrary shape. In this article we shall restrict ourselves to Hall-mobility measurements. It should be noted that Van Der Pauw's theory is only valid if the following four conditions are fulfilled:

(1) The layer must be perfectly flat

(2) The four contacts must be point shaped and placed along the boundary

(3) The layer must be homogeneous
(4) The geometry must be that of a singly connected domain

Only the second condition (point-shaped contacts) is difficult to meet. This article is therefore mainly devoted to the influence of finite contacts on Hall-mobility measurements.

In order to determine the mobility μ_H, a current I is fed through two opposite contacts A and C (Fig. 2). The voltage across the two other contacts B and D is then measured with and without the magnetic field **B**. The difference gives us the so-called Hall voltage. If the magnetic field $\mathbf{B} = 0$, the voltage drop V_1 between the contacts B and D turns out to be

$$V_1 = \int_D^B \mathbf{E} \cdot d\mathbf{r} = \rho \int_D^B \mathbf{J} \cdot d\mathbf{r} \tag{22}$$

When the magnetic field **B** is applied, one finds a voltage V_2 between B and D given by

$$V_2 = \int_D^B \mathbf{E} \cdot d\mathbf{r} = \rho \int_D^B \mathbf{J} \cdot d\mathbf{r} + \rho\mu_H \int_D^B (\mathbf{J} \times \mathbf{B}) \cdot d\mathbf{r} \tag{23}$$

Because the contacts are assumed to be point shaped, the boundary condition $\mathbf{J} \cdot \mathbf{u}_n = 0$ holds along the entire boundary. Since the basic equations and boundary conditions for **J** are unaltered by the magnetic field, one concludes that the current density field **J** remains unchanged. The **J** vector in Eq. (22) is thus the same as in Eq. (23). The Hall voltage is then found to be

$$V_H = V_2 - V_1 = \rho\mu_H \int_D^B (\mathbf{J} \times \mathbf{B}) \cdot d\mathbf{r} \tag{24}$$

with $\mathbf{B} = B\mathbf{u}_z$($\mathbf{u}_z$ directed perpendicular to the Hall plate):

$$V_H = -\rho\mu_H B(I/d) \tag{25}$$

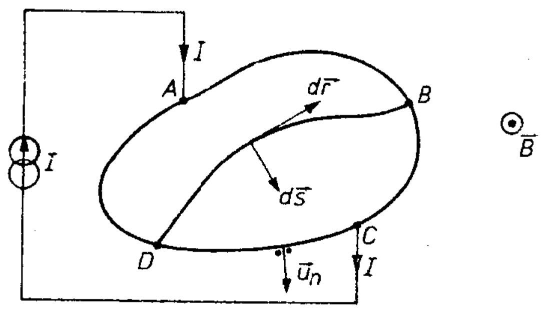

FIG. 2. Hall generator of arbitrary shape placed in a magnetic field **B**.

where d represents the thickness of the layer. Equation (25) enables us to determine the mobility μ_H by measuring the Hall voltage provided that ρ, B, I, and d are known.

IV. Influence of the Geometry on Hall-Mobility Measurements

Equation (25) of Van Der Pauw is only valid if the contacts are point shaped. Actually, Hall generators always show finite contacts, and this will alter the Hall voltage in a still unknown way. It is shown further on in this article that the so-called geometry correction can be calculated provided that the potential problem in a Hall plate is solved.

At this stage it is necessary to emphasize that there are two different kinds of size effects in semiconductor components. The first (and best known) effect is of a purely physical nature. Consider a semiconductor slice that is very thin, in which the mean free path of the charge carriers can become comparable to the thickness. One can easily understand that the mobility will then depend upon the size of the sample (Ghosh, 1961). But in our case the geometry (i.e., finite contacts) has no physical influence on the mobility but will affect the measured Hall voltage. This second kind of size effect is of a purely metrological nature.

We shall now review Section III for the case of finite contacts on a Hall plate. Equations (22) and (23) are still valid; however, as $\mathbf{J}\cdot\mathbf{u}_n = 0$ no longer holds along the entire boundary, the current field $\mathbf{J}$ will change in the presence of a magnetic field. It is then necessary to replace $\mathbf{J}$ by $\mathbf{J} + \Delta\mathbf{J}$ in Eq. (23), where $\Delta\mathbf{J}$ is the change in the current field caused by the magnetic field $\mathbf{B}$. The Hall voltage V_H is then found to be

$$V_H = V_1 - V_2 = \rho\int_D^B \Delta\mathbf{J}\cdot d\mathbf{r} - \rho\mu_H B(I/d) \tag{26}$$

The absolute error $\Delta\mu_H$ introduced by neglecting the influence of the finite contacts is then

$$\Delta\mu_H = (d/BI)\int_D^B \Delta\mathbf{J}\cdot d\mathbf{r} \tag{27}$$

The problem is now to develop a geometry for which the correction (27) is as small as possible in spite of the finiteness of the contacts. One has to find an integration path from D to B in an area where $\Delta\mathbf{J} \approx 0$. This can be done if contacts are placed at the ends of rectangular strips (Fig. 3). From field